Article

Not peer-reviewed version

Automating Laser Vision Correction

Diego de Ortueta *

Posted Date: 4 March 2024

doi: 10.20944/preprints202403.0159.v1

Keywords: automated; transepithelial photorefractive keratectomy; TransPRK; photorefractive keratectomy; aberration free; refraction; AMARIS; Peramis; MS-39; OCT.

 doi:10.20944/preprints202403.0159.v1

Article

Automating Laser Vision Correction

Diego de Ortueta [1,2]

[1] Aurelios Augenzentrum Recklinghausen, Germany; diego.de.ortueta@augenzentrum.org
[2] MD, PhD University Navarra, Spain

Abstract: The purpose of this study is to show an automated laser vision correction (LVC) with the transepithelial refractive keratectomy (TransPRK) surgery technique. Since more surgical steps have been automated over the years, we have standardized the TransPRK technique. We have been using it since 2010. This paper aims to illustrate the processes that are readily applicable to automation. To meet the patient's expectations and ensure that the patient has uncorrected visual acuity at least equal to the preoperative corrected vision with glasses, patient selection is crucial in refractive surgical procedures. One major benefit of automating the surgery is that it can be performed in a similar way by each surgeon or laser correction centre, so once the standard and results are good, these can be performed by different surgeons.

Keywords: automated; transepithelial photorefractive keratectomy; TransPRK; photorefractive keratectomy; aberration free; refraction; AMARIS; Peramis; MS-39; OCT

1. Introduction

The purpose of this study is to demonstrate automated laser vision correction (LVC) using the transepithelial refractive keratectomy (TransPRK) surgery technique.

The principle of keeping it short and simple (KISS) was also found to be keeping it simple and stupid. The KISS principle states that most systems work best if they are kept simple rather than made complicated; therefore, simplicity should be a key goal in design, and unnecessary complexity should be avoided. The phrase has been associated with aircraft engineer Kelly Johnson [1]. The principle is best exemplified by the story of Johnson handing a team of design engineers a handful of tools, with the challenge that they were designing must be repairable by an average mechanic in the field under combat conditions with only these tools. Hence, the "stupid" refers to the relationship between the way things break and the sophistication available to repair them. In case of refractive surgery, we must design a simple workstation to make decisions easier for the physician and repeatable. As an accurate surgery, it will give us excellent results, resulting in satisfied patients with good vision and reducing the number of retreatments.

Because more surgical steps have been automated over time, we have standardized the TransPRK technique. We've been using it since 2010. This paper aims to illustrate processes that are easily automated. The automated TransPRK will be referred to the Schwind AMARIS laser platform (Schwind Eye-Tech Solutions, Kleinostheim, Germany) as a user of this platform. One significant advantage of automating surgery is that it can be performed in a similar manner by each surgeon or laser correction center, so once the standard and results are satisfactory, these can be performed by different surgeons, and therefore good results can be repeated by other surgeons.

2. Patient Selection

2.1. Refraction

When refracting, we employ a completely automated system that includes a digital phoropter, chart projectors, and an automated refractometer.

 doi:10.20944/preprints202403.0159.v1

The process for operating digital refractors is identical to that of manual ones; the adjustments are managed by a digital panel. All refractive data, including the glasses from the lensometer and the objective and subjective refractions, can be updated and saved to the patient's file thanks to the digital system. without any additional redundant data entry or errors in transcription. Our patient file is therefore digital.

We assess astigmatism at 4 mm in diameter using the pyramidal aberrometry system Peramis (CSO-Florence, Italy) [2]. When virgin eyes are chosen for refractive surgery, this astigmatism indicates the axis and amount of astigmatism that needs to be corrected. The amount of sphere is frequently undercorrected for hyperopia and hypercorrected for myopia when the aberrometer is used. The optician uses subjective refraction to determine the quantity of sphere; in myopic eyes, this results in the least amount of negative sphere, and in hyperopic patients, it results in the most accepted sphere with a normal pupil initially and a dilated pupil later. In mydriasis, the calculated sphere represents the physiological amount that needs to be adjusted. In both physiological and mydriasis, the discrepancies between these two refractions shouldn't be greater than 0.75 D. (dioptres). The age of the patient determines how much we can overcorrect this physiological amount. For those under 30, we use the physiological (normal pupil) sphere refraction; for those between 30 and 45, we use the mean sphere, which is the product of the dilated and normal pupil refractions; and for those 45 and beyond, we use the dilated calculated sphere. When the refraction sphere exceeds 0.75 D, we schedule a follow-up consultation to re-evaluate the minimal tolerated sphere in physiological (normal pupil).

2.2. Keratoconus Screening

Thanks to various diagnostic devices that enable us to gather accurate and detailed data, we now have advanced image tools for evaluating the cornea and the anterior morphology of the eye.

We have video topography using the Placido Disc, a very useful unit to measure the anterior corneal shape in an accurate and reproducible manner [3]. With slit-scanning and Scheimpflug imaging, we can reconstruct the three-dimensional structure of the cornea from two-dimensional optical cross sections [4]. We can analyse the cornea thickness, posterior curvature map of the cornea, and anterior chamber depth. With the high-quality spectral domain optical coherence tomography (OCT) [5], we get even more detailed images of the anterior segment. We obtain very high-resolution images and consequently extremely accurate and precise anatomy-topographical data related to several structures of the anterior segment: corneal epithelium, Bowman membrane, corneal stroma, corneal endothelium, posterior corneal curvature, anterior chamber, iris-sclera corneal angle, iris, pupil size and dynamics, and crystalline lens.

With MS-39 (CSO, Florence Italy) we get the combination of videokeratography Placido-disc based, and anterior segment spectral domain OCT [6], we get a detailed panorama of the anterior segment. In contrast to the Scheimpflug we get with the OCT depth information about the epithelium, so that we get precise representation as an epithelium map with a resolution of 3.6 micrometres thanks to spectral domain technology.

To reduce interobserver variability or misdiagnosis we can computerize analysis using machine learning techniques [7]. Posterior corneal curvature and pachymetry data provided by Scheimpflug imaging have been investigated by Ambrosio et al [8], who showed that corneal-thickness spatial profile, corneal-volume distribution, percentage increase in thickness, and percentage increase in volume were different in keratoconic and normal eyes. Combination Placido and OCT can be automated to detect abnormal, keratoconus, suspect keratoconus, myopic post-op or normal relying on the classification by Support Vector Machine (SVM) [7], a machine learning technique screening variations against normality, and since in keratoconus such variations take place in the same position, the bulging area, to report the coincidence of the location of such variations together with corneal epithelium assessment for keratoconus detection in keratoconic eyes, epithelial thickness in the region of the cone has been reported to be thinner than that of normal eyes. We can accurately identify keratoconus and rule out eyes that are not suitable candidates for refractive surgery by using the MS-39 keratoconus screening.

 doi:10.20944/preprints202403.0159.v1

2.3. Treatment Plan

Using the ORK CAM module software, we plan the TransPRK of treatment [9] (SCHWIND eye-tech-solutions, Kleinostheim, Germany) This software serves as a planning tool for excimer laser-assisted refractive procedures. We use the AMARIS laser platform from SCHWIND eye-tech-solutions, Kleinhostheim, Germany. We have a variety of correction options: the aberration-free and the customized. The aberration-free profile treats the lower-order aberrations (LOA) as spherical and cylindrical values. The customized profile uses corneal or ocular wavefront data and can treat lower and higher-order aberrations (HOA).

Correcting the refractive error without causing aberrations is the aim of our corneal surgery in virgin eyes with good visual acuity. Treatment for the great majority of these patients involves the use of the aspheric aberration neutral "Aberration-Free" method[9]. This provides positive outcomes that don't require fixing HOA. Only spherical or cylindrical refractive values are adjusted. Moreover, the treatment does not produce significant HOA that could affect contrast vision or visual acuity. The premise behind the Aberration-Free approach is that eliminating preoperatively existing high-order aberrations is not always beneficial [10]. This is valid for eyes that achieve a high level of visual acuity without experiencing visual problems [9]. Studies on untreated eyes suggest that patients with above-average visual acuity may have some degree of HOA. It was also noted that the patients with the fewest HOA were not usually the ones who had the highest visual acuities. Because the brain uses neural compensation to adapt to aberrations, the patient doesn't need to adjust to new visual circumstances as much.

We suggest using the ocular wavefront data from the PERAMIS system in virgin eyes. When the HOA at 6 mm is less than 0.3 μm, we only treat the LOA, which is the equivalent of treating aberration-free. That means that we filter the HOA and only treat the LOA measured by the wavefront. If the HOA at 6 mm is greater than 0.3 μm, we treat both LOA and HOA in a customized manner. We tailor the treatment, treating both LOA and HOA. The minimize function software for tissue saving in the ORK-CAM can also be used in cases of customized treatments where we treat HOA and wish to use less tissue [11]. In this instance, clinically significant Zernicke polynomials and non-clinically significant aberrations are used by the software to compute the HOA. Abnormalities that are not significant and would preserve tissue are removed and not treated when tissue preservation is the goal.

In most of the cases, we employ the aberration-free profile with the intention to use the ocular wavefront treatment just for treating the LOA. The benefit of using the ocular wavefront is that we can measure cyclotorsion and the astigmatism axis using the same instrument – the aberrometer PERAMIS. Since we have the Peramis pyramidal aberrometer, we have noticed that the astigmatism's axis, measured at 4 mm, is the most accepted astigmatism. We prefer to utilize PERAMIS's computed objective cylinder and the same data for the cyclorotation. Prior to starting the laser treatment, we measure the static cyclorotation between the supine position under the laser and the seated position measured with the PERAMIS aberrometer using an infrared camera. This measurement is performed right before treatment starts, unlike with other refractive intrastromal or intralamellar surgeries. Various studies have computed the impact of cyclotorsion during laser treatment [12–14] showing the refractive error with incorrect cyclotorsion compensation. Additionally, it is possible to select and place the center of the treatment objectively. We employ the Videokeratography information in our case [15]. With the MS-39 we have an instrument with combination of Placido disc and OCT. The Vertex center, or the center of the rings, is obtained from the Placido disc. [15,16] and we utilize this geometrical point as the treatment's center and point of reference. The offset is the distance between the pupil center and the vertex of the cornea. We use the full offset. Some authors use 2/3 of the offset [17]. In the case that we treat HOA as we measured it with the aberrometer, and the measurement implies the pupil, the software centers the treatment of the HOA on the pupil center. So, the surgeon can determine where to center the LOA in our case with the offset on the corneal vertex, but the HOA, if treated, is centered on the pupil center based on the measurement of the aberrometer. We also have two different ablation strategies: the symmetric strategy with a concentric treatment with the vertex and the asymmetrical strategy where the treatment is concentric to the pupil but the center is the

 doi:10.20944/preprints202403.0159.v1

vertex of the cornea, by doing this, tissue is spared from the need to increase the optical zone. Since the TransPRK allows us to increase the optical zone, we prefer the symmetrical approach [18] because the postoperative topography shows greater symmetry. We advise using an optical zone that is at least twice the offset distance in addition to the pupil in mesopic for the minimum optical zone. Since the software can now extend the treatment by 1mm from the measurement, we should attempt to measure with the aberrometer under mesopic conditions and with a large pupil. The ORK-CAM also computes the minimal optical zone (OZ). The transition zone is also computed by the software using the optical zone and refraction as inputs. inputs. So we get in one file from the OW the refraction, the infrared photography for statical cyclotorsion, the HOA are filtered if we treat taberration-free (in the majority of cases, this is the case). From the placido rings, we get: the position of the vertex in relation to the limbus and pupil; the keratometry values; from the OCT, the epithelium thickness at the center and the mean thickness at a 4 mm radius; the total pachymetry; and the standard optical zone of 6.7 mm, which can be changed to a bigger oz if needed; the transition zone is calculated by the software.

2.4. Laser Platform

We use of the SCHWIND AMARIS 1500Hz RS laser, which has a Super-Gaussian beam profile and a small 0.54-millimetre spot size using two fluences the higher fluence with 500mj/cm^2 and the low fluence with 300mJ/cm^2 (SCHWIND eye-tech-solutions, Kleinhostheim, Germany). The improved spot overlap matrix prevents vacancies and corneal roughness by an accurate reproduction of the computed ablation volume. The system can shorten the ablation time while keeping the same tissue conditions throughout thanks to the 1050 Hz ablation's high speed. The Intelligent Thermal Effect Control (ITEC) on the SCHWIND AMARIS laser systems guards against damage to the surrounding corneal tissue even at extremely high ablation speeds. The ITEC algorithm [19] distributes the laser pulses in a way that is both thermally optimized and dynamically adjusted, allowing the cornea to cool down sufficiently. This enables faster approach of a position that has already cooled by subsequent pulses. Our in vivo thermal measurements[23] demonstrate that the cornea's temperature rise is always significantly less than 40°, which is thought to be critical for corneal tissue denaturation, and is never greater than 5°. The laser systems actively compensate for eye movements with an average latency of about 1.6 ms. An integrated eye tracker monitors the eye's position 1,050 times per second. The camera, scanner, electronics, and software all work together to provide an overall reaction time for the AMARIS that is typically less than 3 ms. The precision with which the laser spots are positioned and the eye is centred determine the accuracy of the results of a refractive treatment [20]. Apart from the pupil, the limbus is also detected by the eye tracker. Unlike the pupil's diameter, the limbus's size is constant. Because of this, the limbus is used as a reference for ablation, preserving the original ablation centre throughout the course of treatment. This enables us to select the exact location of the ablation centre, which stays in that position the entire time because the laser system tracks the movement of the pupil in relation to the limbus.

Automatic pupil size monitoring during static cyclotorsion control provides extra security [13]. To maintain the same pupil size at the beginning of treatment as it did during the preoperative exam, which is when the diagnostic data was gathered, the lighting is automatically adjusted. During ablation, changes in corneal curvature combined with a non-normal laser beam incidence result in efficiency and reflection losses [21]. By taking these losses into account, the ORK-CAM software makes sure that the necessary ablation volume is accurately removed. As a necessary result, the patient's refractive deficit and the keratometry readings for both meridians are imported from the videokeratography into the ORK-CAM software at the proper vertex distance.

2.5. Pearl – TransPRK

Transepithelial Photorefractive Keratectomy (TransPRK), a no-touch, all-laser surface ablation, is an advanced method of surface treatments [22,23]. The laser system thus ablates the regenerating surface of the eye, the epithelium, and then the stroma. When using the TransPRK, treating an eye's surface doesn't require touching the eye with an instrument. The ORK-CAM includes distinct tissue

 doi:10.20944/preprints202403.0159.v1

ablations for the stroma and the epithelium [24] in the computation to avoid unintended refractive effects during epithelium ablation. Because the epithelium is known to be thicker in the periphery, the software ablates with a central diameter of 55 μm and a peripheral diameter of 65 μm, or 8.0 mm. Even a small deviation from this averaged value of epithelial thickness will not lead to an over- or undercorrection; instead, a thinner or thicker epithelium will result in a slightly deeper ablation or a smaller optical zone [25]. In both situations, the desired refractive change and curvature shape will be achieved. Directly beneath the area where the epithelium is removed by laser is the total zone of ablation (TZ), which is the total of the transition zone and the chosen optical zone (OZ) (TZ). Due to the smaller wound surface compared to manual PRK, the healing process takes one or two days less. [26]. In addition, a single procedure is used to ablate both the stroma and the epithelium. This significantly reduces the total amount of time needed for treatment and diminishes the possibility of corneal dehydration [27]. We are able to precisely measure the epithelium and carry out a customized epithelium treatment with the MS-39 (CSO, Florence, Italy) [28]. In order to achieve even more precise epithelium ablation than with the standard laser ablation software, which has 55μm at the center and 65μm at 8mm, we import the data of the central epithelium as well as the mean epithelium thickness at 8mm of diameter. When we consider small amounts of refractive error as being under two dioptres of myopia [25], this becomes especially interesting.

3. Material

To demonstrate that an automated TransPRK gives good results, we performed a retrospective study of a consecutive group of myopic eyes treated in Aurelios Recklinghausen, Germany, with at least a follow-up of 3 months. In all the cases, the eyes were virgin eyes with a good visual acuity (at least 0.8) without any other clinically relevant change in the eye or systemic disease that could affect the eye. The mean preoperatively spherical equivalent was -3.52 dioptres (D) with a range between -0.75D and -7D and a mean preoperatively astigmatism of 0.98D with a range of -2.75D. In all the cases, the same surgeon, DdO, treated with TransPRK. As all the cases had good visual acuity, we treated with the aberration-free profile. As described before, we created one file of a patient under the automated phoropter. The measured astigmatism by the PERAMIS was imported, and the optician calibrated the sphere as described. The file of the aberrometry from the PERAMIS was exported after adjusting the sphere as measured by the optician. From this file of ocular aberrometry, we filtered the HOA to treat only the LOA (sphere and cylinder). With this file, we also got the cyclotorsion information for the laser platform to adjust the static cyclotorsion of the eye from sitting to supine position. From the MS-39, we had a second file. Here we get information on the keratometry, the position of the vertex of the cornea in relation to the limbus, the central pachymetry, and the epithelial map with the mean centre thickness and the mean peripheral thickness. The MS-39 also has software to calculate if the patient has a normal cornea or if keratoconus is suspected. With these files, we get one ORK CAM file (see Figures 1–3). In this case, the software also calculates if the residual stroma is enough (at least 250 μm). With this file, we begin the treatment under the laser. After the calibration, we use infrared photography to identify the eye. If we have the correct patient, the software will recognize the eye and correct the static cyclotorsion. After that, the ablation occurs in these cases between 22 seconds and 59 seconds, depending on the refractive error. The results in this group of eyes were very good, with a postoperative SEQ of -0.02D and a mean postoperative cylinder of -0.11D. For more details, see Table 1.

Preprints.org (www.preprints.org) | NOT PEER-REVIEWED | Posted: 4 March 2024 doi:10.20944/preprints202403.0159.v1

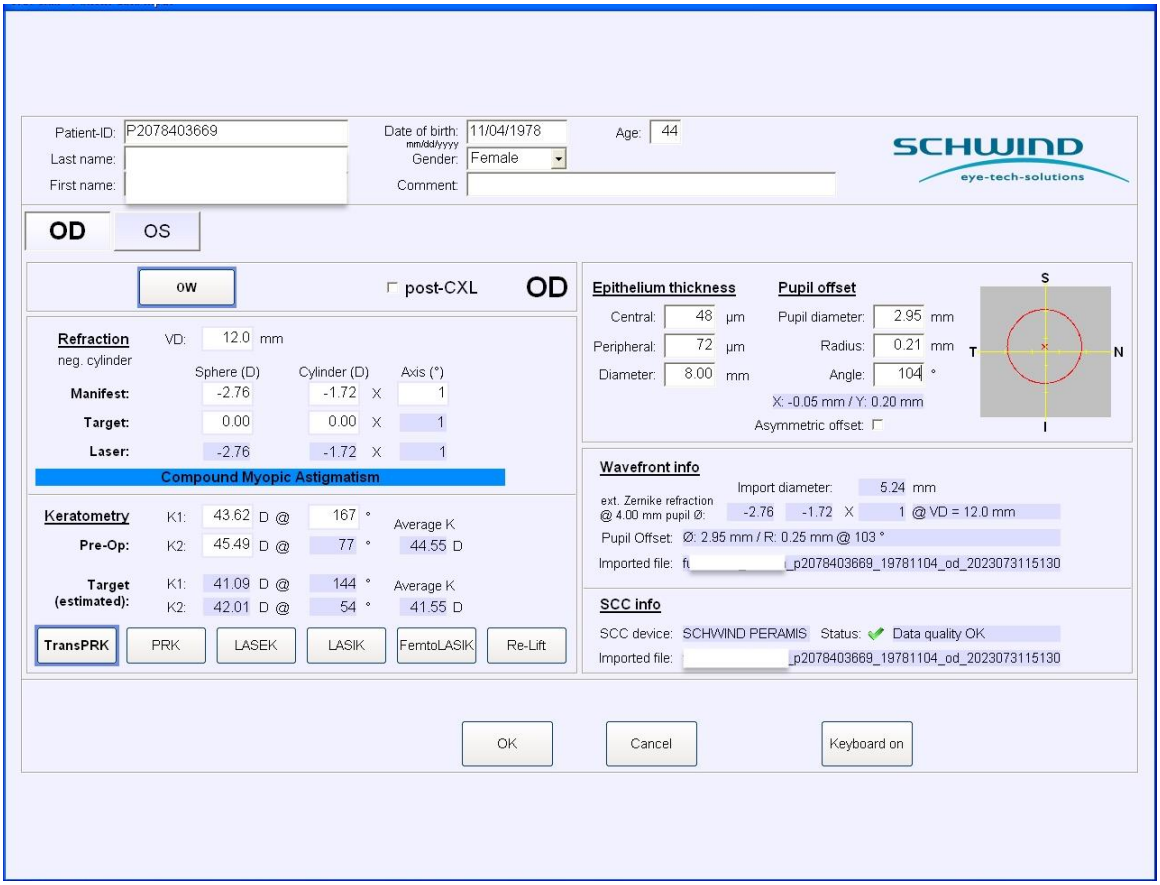

Figure 1. Created file with the ORK-CAM software. The patient has one number that is also identical to the imported files. Using the Peramis aberrometer, we were able to obtain the refraction and the statistical cyclotorsion (SCC). Additionally from the MS-39 we obtained the keratometry data, the epithelium thickness, and the pupil offset for the centration.

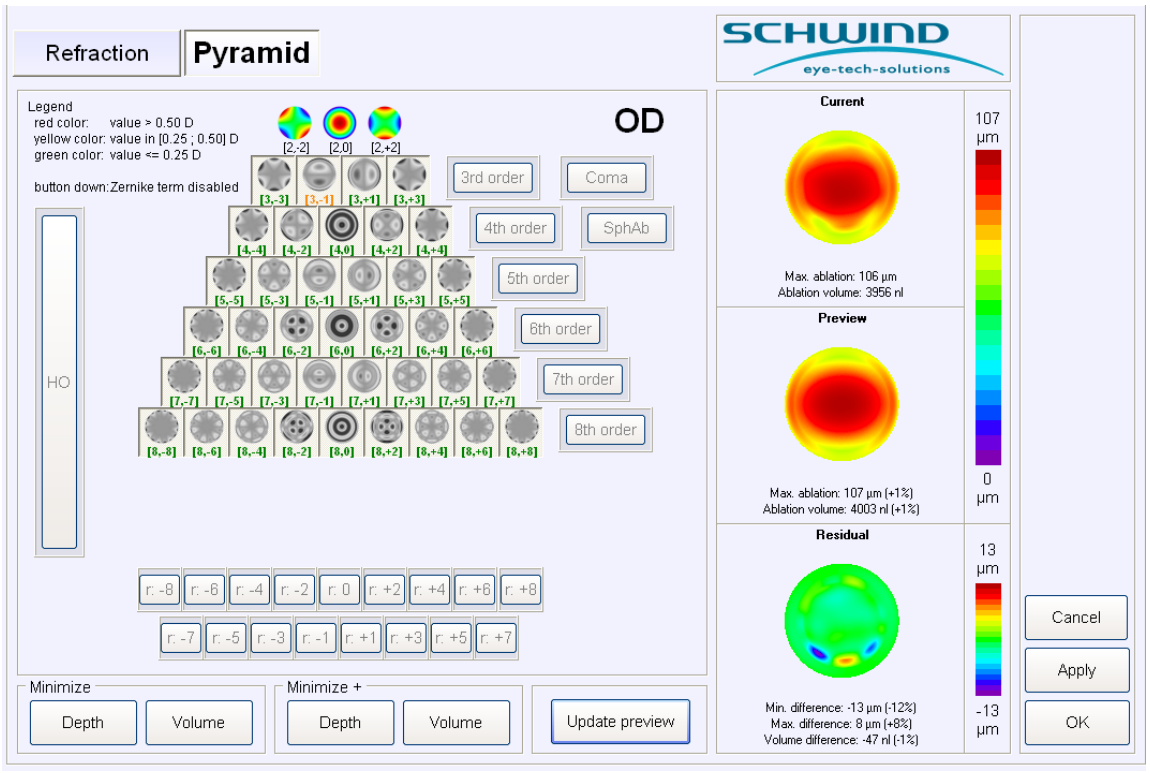

 doi:10.20944/preprints202403.0159.v1

Figure 2. From the aberrometry, we get information on the lower-order aberrations (LOA) and the higher-order aberrations (HOA). As we want only to treat the LOA, we filter the HOA. At the right top is the profile with HOA and LOA; in the right middle is the treatment of the LOA; and at the right bottom is the residual untreated HOA.

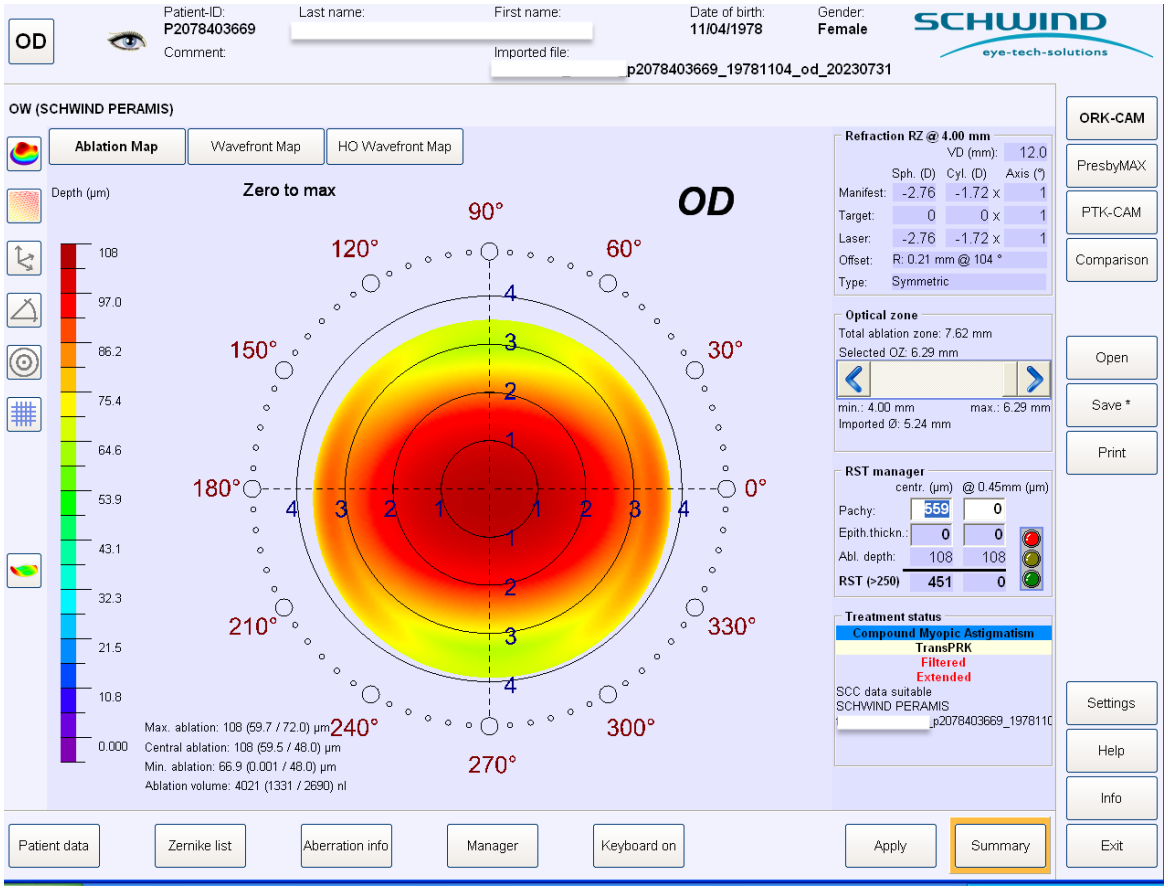

Figure 3. The ablation profile map that is imported to the laser platform The optical zone (OZ) and the transition zone (TZ) are calculated based on the measurement in mesopic conditions of the Peramis aberrometry. Residual thickness is also shown.

No one loses more than one line of corrected distance visual acuity. The refractive outcome was in 95% of the cases under 0.5D and 100% of the cases under 1D. The refractive astigmatism was in 98% of the cases under 0.5D and in 100% of the cases under 1D. The predictability was very good, with a coefficient of regression of 0.98, which is very close to one, showing excellent predictability. The average deviation from the attempted versus achieved SEQ was -0.03 D. Further details are shown in Figures 4–6.

Preprints.org (www.preprints.org) | NOT PEER-REVIEWED | Posted: 4 March 2024 doi:10.20944/preprints202403.0159.v1

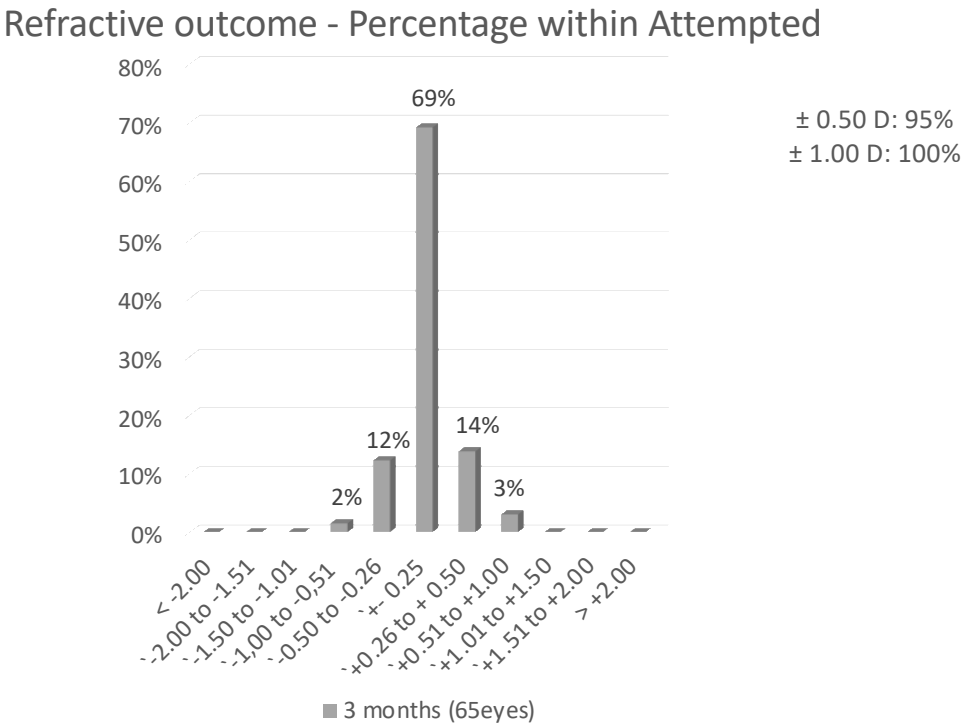

Figure 4. Reffractive outcome in spherical equivalent (SEQ) after 3 months of the TransPRK treatment.

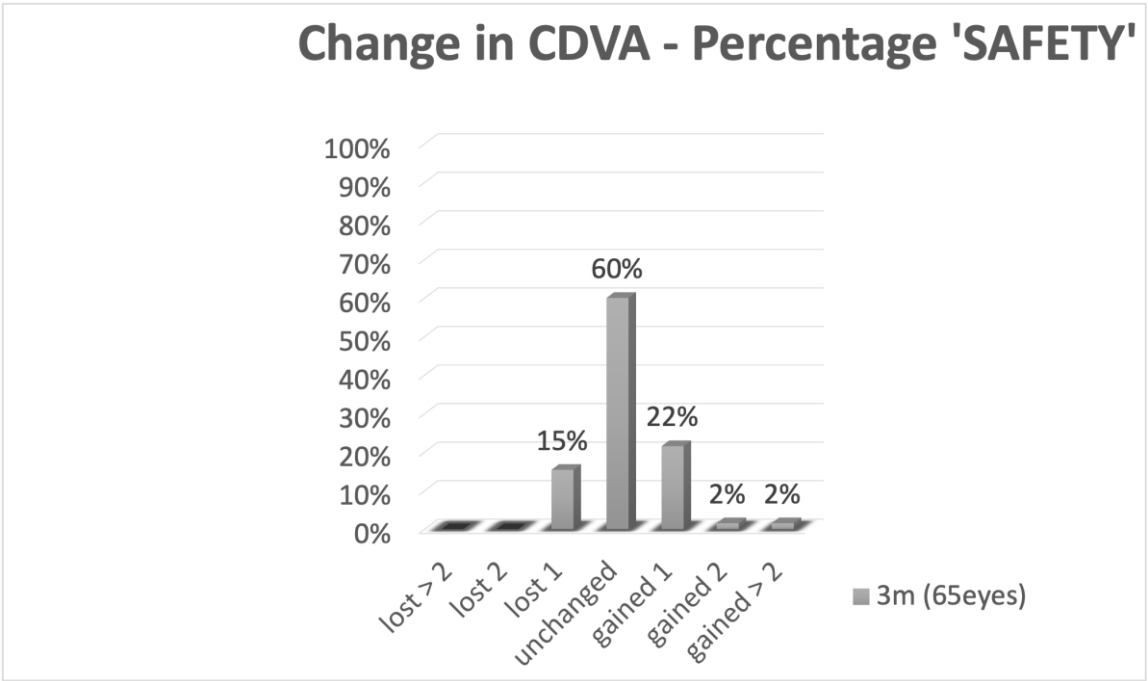

Figure 5. Safety of the TransPRK procedure. No eye loose 2 or more lines of Snellen vision.

 doi:10.20944/preprints202403.0159.v1

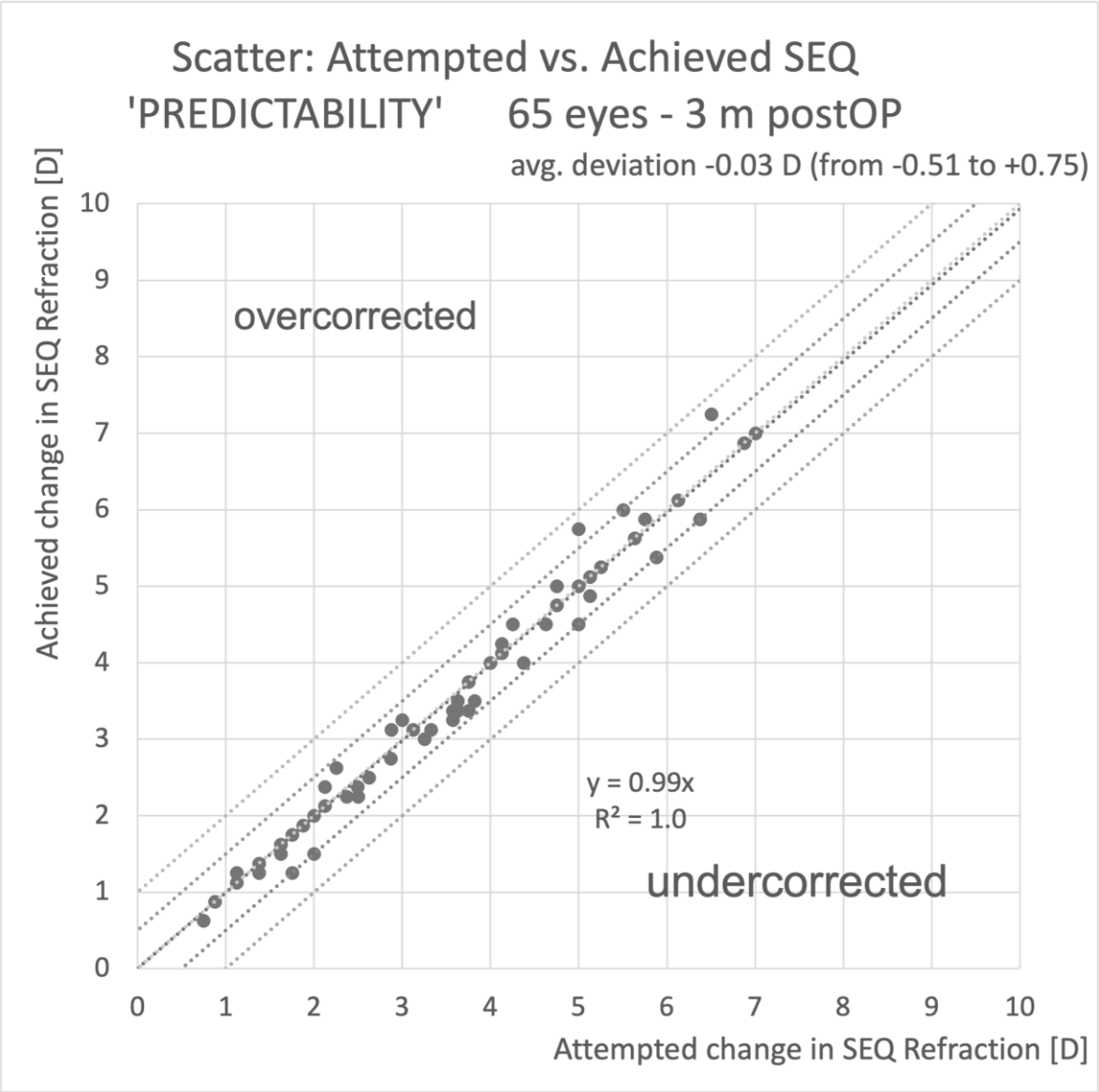

Figure 6. Predictability showing attempted correction versus achieved correction. The regression coefficient y s near to 1, showing a good predictability.

4. Discussion

When it comes to refractive surgery, it is essential to screen candidates before they undergo corneal refractive surgery to avoid complications. We have tools and screening methods that utilize machine learning techniques [29–31] in order to determine whether or not corneal refractive surgery is appropriate for the patient. Through the use of digital workflows, we are also able to obtain more accurate and reliable measurements of refractive errors [32]. Our recommendation also includes the utilization of a single digital file for each individual patient, with the objective of minimizing the number of transcription errors.

We suggest a simplified way to treat refractive errors with advanced surface ablation TransPRK. We have shown that a most of the processes can be automated as astigmatism from the Aberrometer. Other authors also propose to use the data of the aberrometry but then using a nomogram [33], we have found that this is not necessary with the pyramidal aberrometer. The pyramidal aberrometer shows 0.2D of repeatability for astigmatism measured at 5mm of pupil diameter [34]. Comparing pyramidal aberrometry to Hartmann-Shack aberrometry, there are theoretical advantages in terms of higher dynamic range and higher sampling density [34].

 doi:10.20944/preprints202403.0159.v1

Furthermore, it is suggested that the optometrist should only have control over the sphere; the patient's age determines how much we overcorrect this physiological amount. The physiological pupil sphere refraction is used for individuals under 30, the mean sphere, which is the product of the dilated and normal pupil refractions, is used for individuals between 30 and 45, and the dilated calculated sphere is used for individuals 45 and over. The decision of which kind of treatment Aberration-free, Ocular wavefront or Corneal wavefront (topographic guided) must be done by the surgeon, in most of the cases in virgin eyes we can use the aberration-free or in a similar way the OW filtering the aberrations and treating only the LOA with allows us to get an automated file. In cases of complication, we must decide per case, and this cannot be completely automated as the surgeon is the responsible and not the laser system. But in the standard case of virgin eyes, we have shown that a lot of data is created in one file and imported before the treatment, allowing us to perform an automated surgery. This data is imported together with the MS-39 data that gives us the epithelium thickness at the centre and at the periphery, the pachymetry data, the keratometry data, the cyclotorsion data as limbus and pupil centre and the position of the vertex in relation to these two geometrical data.

We have obtained with this automated technique at least results that are comparable to those that have been published in the past. The effectiveness and safety of the TransPRK procedures have been extensively demonstrated to be a successful technique for treating myopia and myopic astigmatism [22,35–39].

Limitations of this study include the non-comparative nature of the study and its utilization of prior research to evaluate findings pertaining to measurement repeatability in relation to manifest refraction and treatment outcomes. As a result, we are unable to address potential benefits for subjective visual outcomes between aberrometry guided semi-automated TransPRK and traditional TransPRK treatment.

5. Conclusion

We have introduced a standard procedure that automates refractive surgery with TransPRK using the PERAMIS Aberrometer for the refraction and, if required, to treat HOA. From the anterior OCT and videokeratography with the MS-39, we export the data for centration, keratometry reading, epithelium thickness, and cyclotorsion. All these measurements are imported into a file, which enables them to be treated automatically.

Author Contributions: Conceptualization, methodology, validation, writing—original draft preparation, review and editing Dd=

Funding: This research received no external funding

Institutional Review Board Statement: the study did not require ethical approval as it is retrospective.

Conflicts of Interest DdO is Consultant for SCWIND eye-tech-solutions.

References

1. The Minneapolis Star. Published online February 12, 1938.
2. Singh NK, Jaskulski M, Ramasubramanian V, et al. Validation of a Clinical Aberrometer Using Pyramidal Wavefront Sensing. *Optom Vis Sci*. 2019;96(10):733-744. doi:10.1097/OPX.0000000000001435
3. Liu Z, Huang AJ, Pflugfelder SC. Evaluation of corneal thickness and topography in normal eyes using the Orbscan corneal topography system. *Br J Ophthalmol*. 1999;83(7):774-778. doi:10.1136/bjo.83.7.774
4. Konstantopoulos A, Hossain P, Anderson DF. Recent advances in ophthalmic anterior segment imaging: a new era for ophthalmic diagnosis? *Br J Ophthalmol*. 2007;91(4):551-557. doi:10.1136/bjo.2006.103408
5. Li Y, Meisler DM, Tang M, et al. Keratoconus diagnosis with optical coherence tomography pachymetry mapping. *Ophthalmology*. 2008;115(12):2159-2166. doi:10.1016/j.ophtha.2008.08.004

6. Savini G, Schiano-Lomoriello D, Hoffer KJ. Repeatability of automatic measurements by a new anterior segment optical coherence tomographer combined with Placido topography and agreement with 2 Scheimpflug cameras. *Journal of Cataract & Refractive Surgery*. 2018;44(4). https://journals.lww.com/jcrs/Fulltext/2018/04000/Repeatability_of_automatic_measurements_by_a_new.10.aspx
7. Arbelaez MC, Versaci F, Vestri G, Barboni P, Savini G. Use of a Support Vector Machine for Keratoconus and Subclinical Keratoconus Detection by Topographic and Tomographic Data. *Ophthalmology*. 2012;119(11):2231-2238. doi:10.1016/j.ophtha.2012.06.005
8. Luz A, Lopes B, Salomão M, Ambrósio R. Application of corneal tomography before keratorefractive procedure for laser vision correction. *J Biophotonics*. 2016;9(5):445-453. doi:10.1002/jbio.201500236
9. Arba-Mosquera S, de Ortueta D. Analysis of optimized profiles for "aberration-free" refractive surgery. *Ophthalmic Physiol Opt*. 2009;29(5):535-548. doi:10.1111/j.1475-1313.2009.00670.x
10. Artal P, Chen L, Fernández EJ, Singer B, Manzanera S, Williams DR. Neural compensation for the eye's optical aberrations. *Journal of Vision*. 2004;4(4):4. doi:10.1167/4.4.4
11. Arba Mosquera S, de Ortueta D. Optimized Zernike Term Selection in Customized Treatments for Laser Corneal Refractive Surgery: Case Report. *J Refract Surg*. 2010;27(2):148-152. doi:10.3928/1081597X-20100224-01
12. Adib-Moghaddam S, Soleyman-Jahi S, Tofighi S, et al. Factors Associated With Ocular Cyclotorsion Detected by High-Speed Dual-Detection Eye Tracker During Single-Step Transepithelial Photorefractive Keratectomy. *J Refract Surg*. 2018;34(11):736-744. doi:10.3928/1081597X-20181001-01
13. Arba-Mosquera S, Merayo-Lloves J, de Ortueta D. Clinical effects of pure cyclotorsional errors during refractive surgery. *Invest Ophthalmol Vis Sci*. 2008;49(11):4828-4836. doi:10.1167/iovs.08-1766
14. Arba-Mosquera S, Aslanides IM. Analysis of the effects of Eye-Tracker performance on the pulse positioning errors during refractive surgery. *Journal of Optometry*. 2012;5(1):31-37. doi:10.1016/j.optom.2011.11.002
15. de Ortueta D, Schreyger FD. Centration on the cornea vertex normal during hyperopic refractive photoablation using videokeratoscopy. *J Refract Surg*. 2007;23(2):198-200.
16. Mosquera SA, Verma S, McAlinden C. Centration axis in refractive surgery. *Eye and Vis*. 2015;2(1):4. doi:10.1186/s40662-015-0014-6
17. Kermani O. Automated visual axis alignment for refractive excimer laser ablation. *J Refract Surg*. 2006;22(9 Suppl):S1089-1092. doi:10.3928/1081-597X-20061102-15
18. De Ortueta D, Von Rüden D, Arba Mosquera S. Symmetric offset versus asymmetric offset ablation with transepithelial refractive keratectomy. *BMC Ophthalmol*. 2023;23(1):219. doi:10.1186/s12886-023-02971-9
19. Brunsmann U, Sauer U, Dressler K, Triefenbach N, Mosquera SA. Minimisation of the thermal load of the ablation in high-speed laser corneal refractive surgery: the 'intelligent thermal effect control' of the AMARIS platform. *null*. 2010;57(6):466-479. doi:10.1080/09500341003710492
20. Arba-Mosquera S, Hollerbach T. Ablation Resolution in Laser Corneal Refractive Surgery: The Dual Fluence Concept of the AMARIS Platform. *Advances in Optical Technologies*. 2010;2010:1-13. doi:10.1155/2010/538541
21. Arba-Mosquera S, de Ortueta D. Geometrical analysis of the loss of ablation efficiency at non-normal incidence. *Opt Express*. 2008;16(6):3877-3895. doi:10.1364/oe.16.003877
22. Aslanides IM, Kymionis GD. Trans advanced surface laser ablation (TransPRK) outcomes using SmartPulseTechnology. *Cont Lens Anterior Eye*. 2017;40(1):42-46. doi:10.1016/j.clae.2016.11.004
23. Aslanides IM, Padroni S, Arba Mosquera S, Ioannides A, Mukherjee A. Comparison of single-step reverse transepithelial all-surface laser ablation (ASLA) to alcohol-assisted photorefractive keratectomy. *Clin Ophthalmol*. 2012;6:973-980. doi:10.2147/OPTH.S32374
24. Seiler T, Kriegerowski M, Schnoy N, Bende T. Ablation rate of human corneal epithelium and Bowman's layer with the excimer laser (193 nm). *Refract Corneal Surg*. 1990;6(2):99-102.
25. de Ortueta D, von Rüden D, Arba-Mosquera S. Comparison of Refractive and Visual Outcomes after Transepithelial Photorefractive Keratectomy (TransPRK) in Low versus Moderate Myopia. *Photonics*. 2021;8(7):262. doi:10.3390/photonics8070262
26. Lee HK, Lee KS, Kim JK, Kim HC, Seo KR, Kim EK. Epithelial healing and clinical outcomes in excimer laser photorefractive surgery following three epithelial removal techniques: mechanical, alcohol, and excimer laser. *Am J Ophthalmol*. 2005;139(1):56-63. doi:10.1016/j.ajo.2004.08.049

27. de Ortueta D, von Rüden D, Magnago T, Arba Mosquera S. Influence of stromal refractive index and hydration on corneal laser refractive surgery. *J Cataract Refract Surg*. 2014;40(6):897-904. doi:10.1016/j.jcrs.2013.07.050
28. de Ortueta D, von Rüden D, Arba-Mosquera S. Customized versus Standard Epithelium Profiles in Transepithelial Photorefractive Keratectomy. *Optics*. 2021;2(4):266-275. doi:10.3390/opt2040025
29. Yoo TK, Ryu IH, Lee G, et al. Adopting machine learning to automatically identify candidate patients for corneal refractive surgery. *npj Digit Med*. 2019;2(1):59. doi:10.1038/s41746-019-0135-8
30. Ting DSW, Pasquale LR, Peng L, et al. Artificial intelligence and deep learning in ophthalmology. *Br J Ophthalmol*. 2019;103(2):167-175. doi:10.1136/bjophthalmol-2018-313173
31. Ang M, Gatinel D, Reinstein DZ, Mertens E, Alió Del Barrio JL, Alió JL. Refractive surgery beyond 2020. *Eye*. 2021;35(2):362-382. doi:10.1038/s41433-020-1096-5
32. Ohlendorf A, Leube A, Wahl S. Advancing Digital Workflows for Refractive Error Measurements. *JCM*. 2020;9(7):2205. doi:10.3390/jcm9072205
33. Allan BD, Hassan H, Ieong A. Multiple regression analysis in nomogram development for myopic wavefront laser in situ keratomileusis: Improving astigmatic outcomes. *Journal of Cataract and Refractive Surgery*. 2015;41(5):1009-1017. doi:10.1016/j.jcrs.2014.08.042
34. Frings A, Hassan H, Allan BD. Pyramidal Aberrometry in Wavefront-Guided Myopic LASIK. *J Refract Surg*. 2020;36(7):442-448. doi:10.3928/1081597X-20200519-03
35. Kaluzny BJ, Cieslinska I, Mosquera SA, Verma S. Single-Step Transepithelial PRK vs Alcohol-Assisted PRK in Myopia and Compound Myopic Astigmatism Correction. *Medicine (Baltimore)*. 2016;95(6):e1993. doi:10.1097/MD.0000000000001993
36. Antonios R, Abdul Fattah M, Arba Mosquera S, Abiad BH, Sleiman K, Awwad ST. Single-step transepithelial versus alcohol-assisted photorefractive keratectomy in the treatment of high myopia: a comparative evaluation over 12 months. *Br J Ophthalmol*. 2017;101(8):1106-1112. doi:10.1136/bjophthalmol-2016-309409
37. de Ortueta D, von Rüden D, Verma S, Magnago T, Arba-Mosquera S. Transepithelial Photorefractive Keratectomy in Moderate to High Astigmatism With a Non-wavefront–Guided Aberration-Neutral Ablation Profile. *J Refract Surg*. 2018;34(7):466-474. doi:10.3928/1081597X-20180402-04
38. Adib-Moghaddam S, Soleyman-Jahi S, Sanjari Moghaddam A, et al. Efficacy and safety of transepithelial photorefractive keratectomy. *J Cataract Refract Surg*. 2018;44(10):1267-1279. doi:10.1016/j.jcrs.2018.07.021
39. Fadlallah A, Fahed D, Khalil K, et al. Transepithelial photorefractive keratectomy: clinical results. *J Cataract Refract Surg*. 2011;37(10):1852-1857. doi:10.1016/j.jcrs.2011.04.029